Tomographic imaging of all orthogonal components of the displacement field in weakly scattering materials using Wavelength Scanning Interferometry

P. D. Ruiz
Wolfson School of Mechanical and Manufacturing Engineering
Loughborough University, UK

Good, but not enough

Detection and sizing of delaminations in CFRP plates using temporal phase shifting speckle interferometry

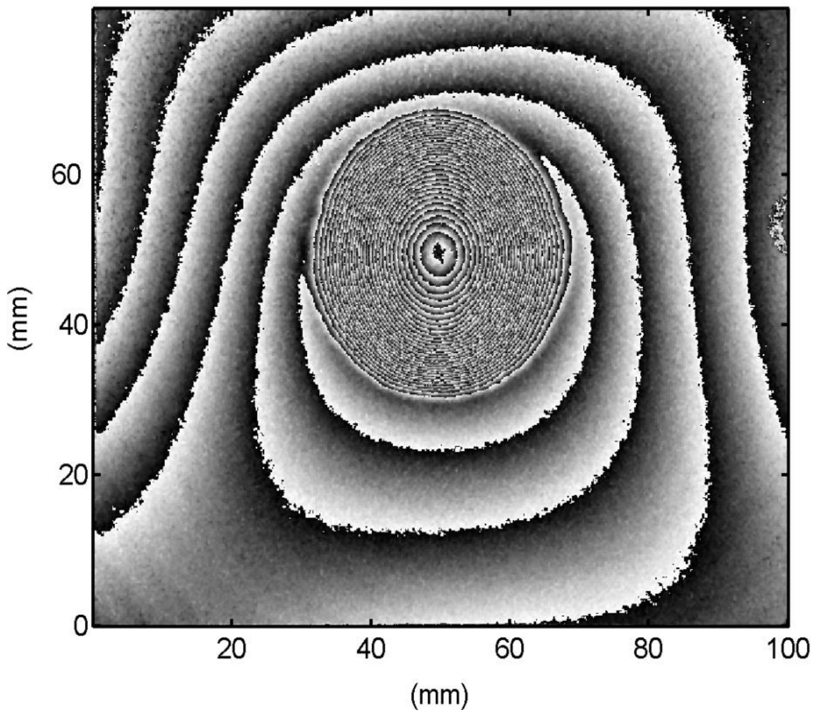

Wrapped phase

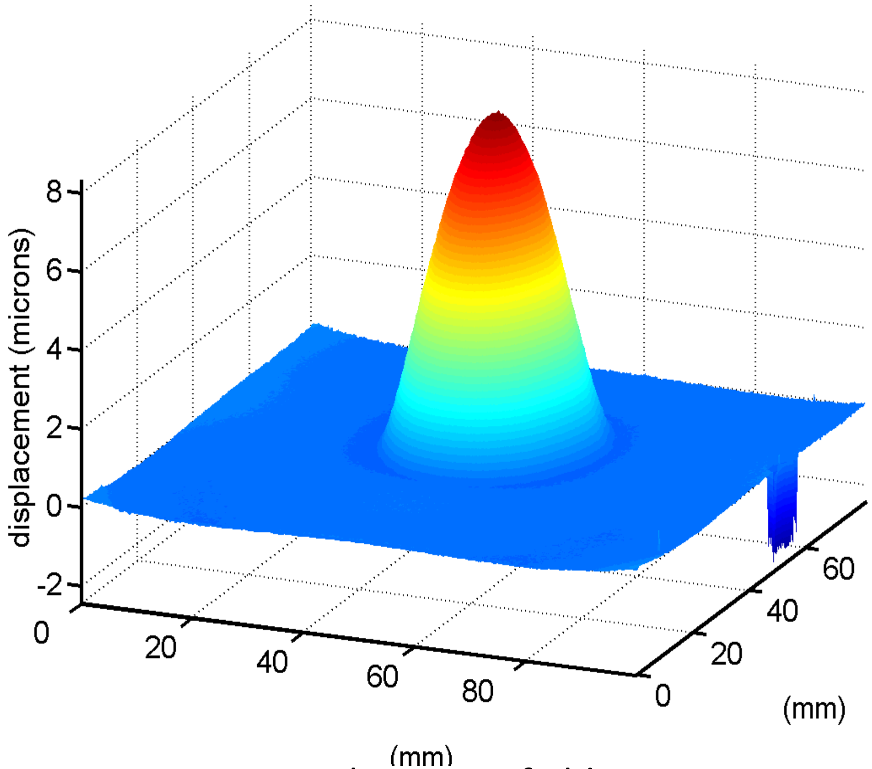

Displacement field

- Internal structure and deformation difficult to estimate through inverse methods
- **e.g.**: solution for **size** and **depth** of delamination is not unique

Maranon, A., et al., Composites Science and Technology, 2007. **67**(13): p. 2817-2826.

Solution for size and depth not unique

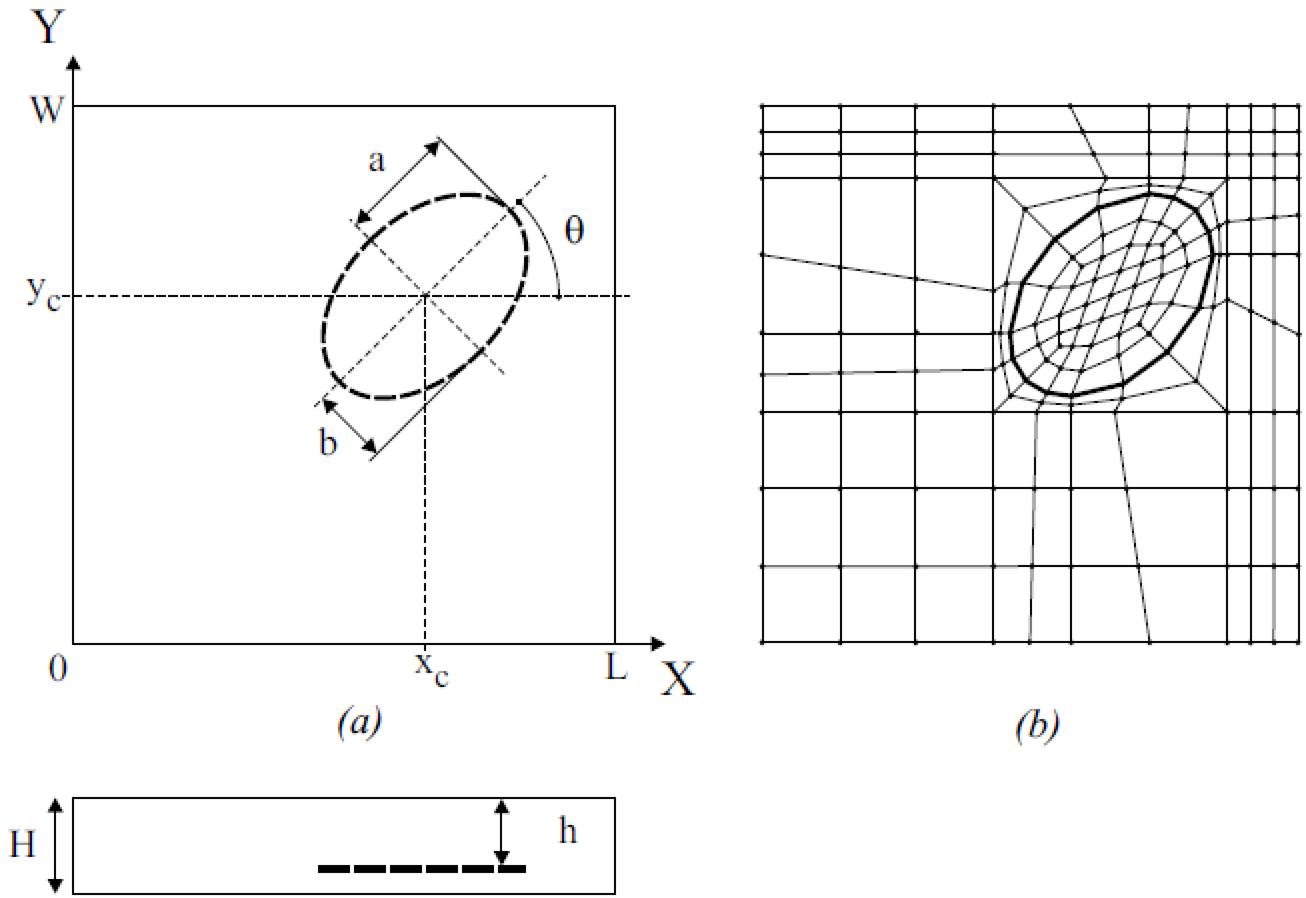

- Finite element analysis and genetic algorithms used to find solution iteratively

Optical Coherence Tomography

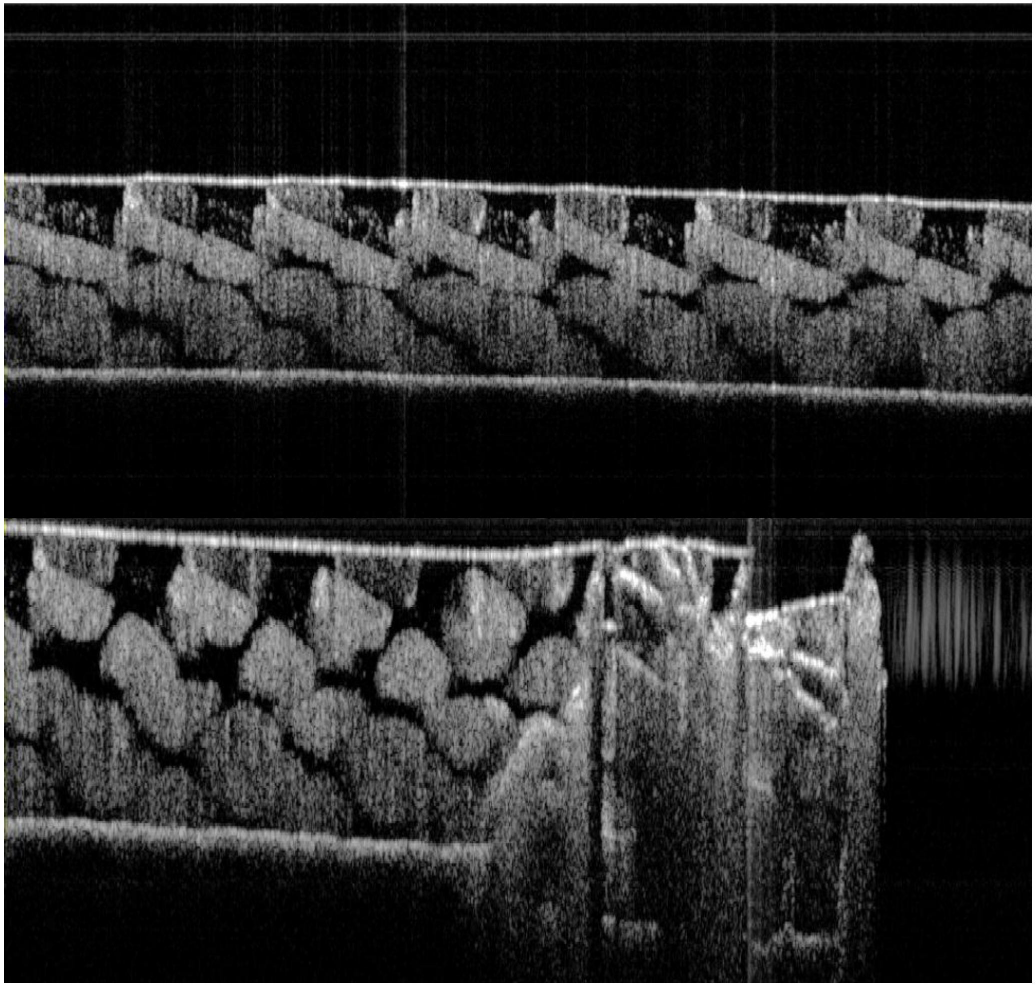

Cross section of glass fibre reinforced composite plates

Identification of mechanical properties

Measured loads and deformations

↓

Full field Identification techniques
(e.g. Finite Element Method Updating,
Virtual Fields Method)

↓

material properties
(e.g. elastic modulus, Poisson’s ratio, stiffness)
Position dependent!

Full strain field required!

So…

First attempts: LCI

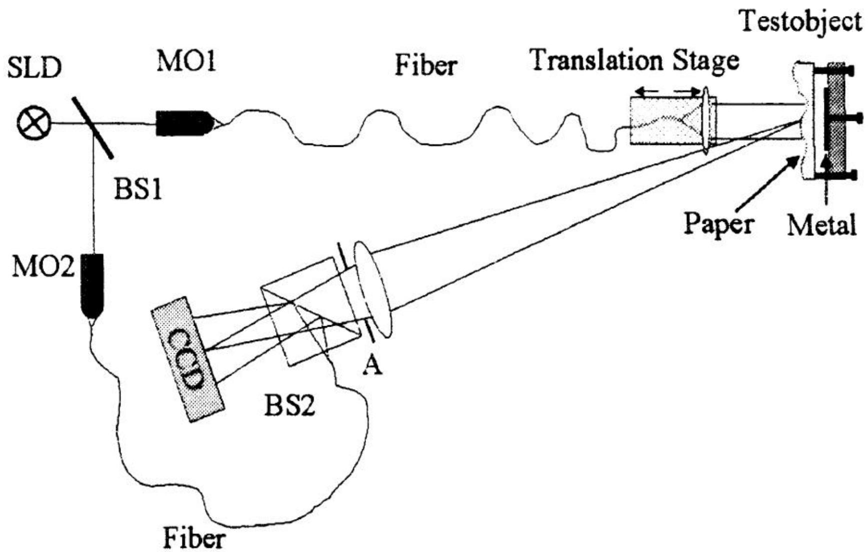

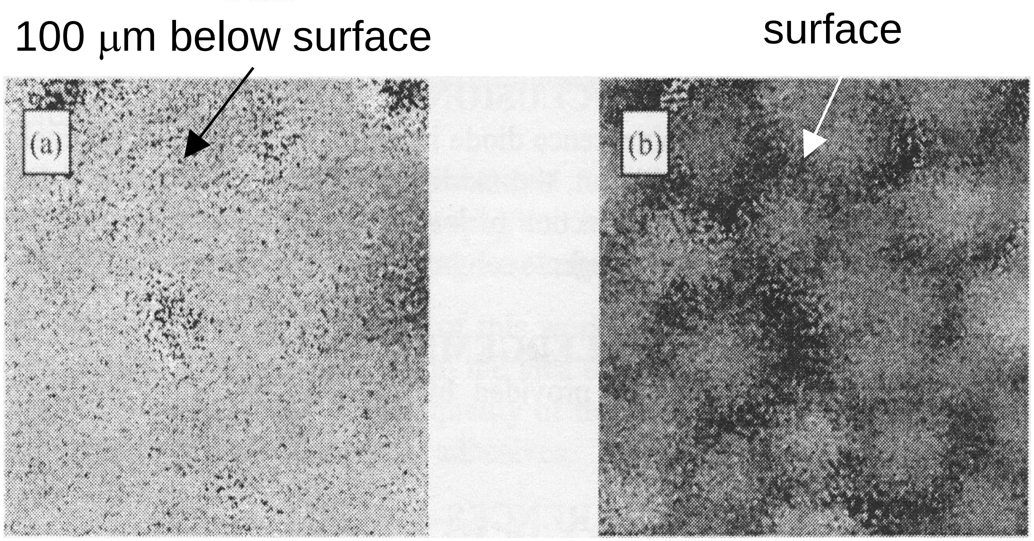

LOW COHERENCE INTERFEROMETRY

- ‘Coherence gate’ selects a slice within the sample
- Standard “digital speckle pattern interferometry”
- Phase maps encode out-of-plane displacements
- Application: paint loss in terracotta soldiers (humidity change 68%→73%)

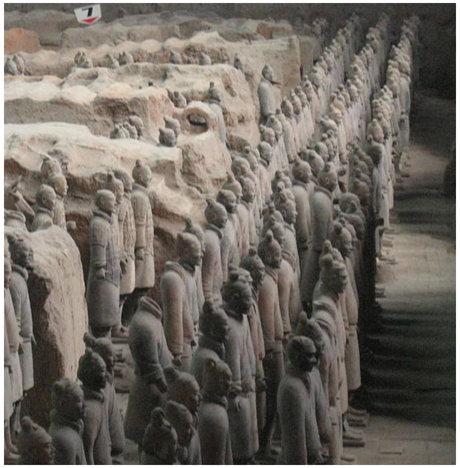

G. Gülker and A. Kraft, in *Speckle Metrology 2003*, SPIE Vol. 4933, p. 53 (2003)

Wavelength scanning interferometry

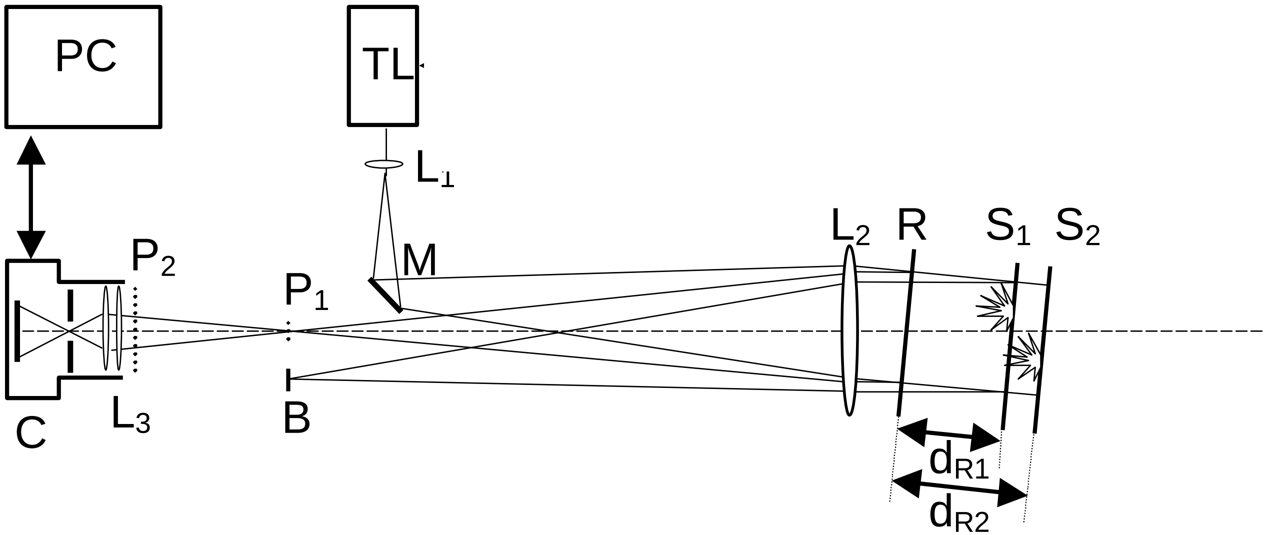

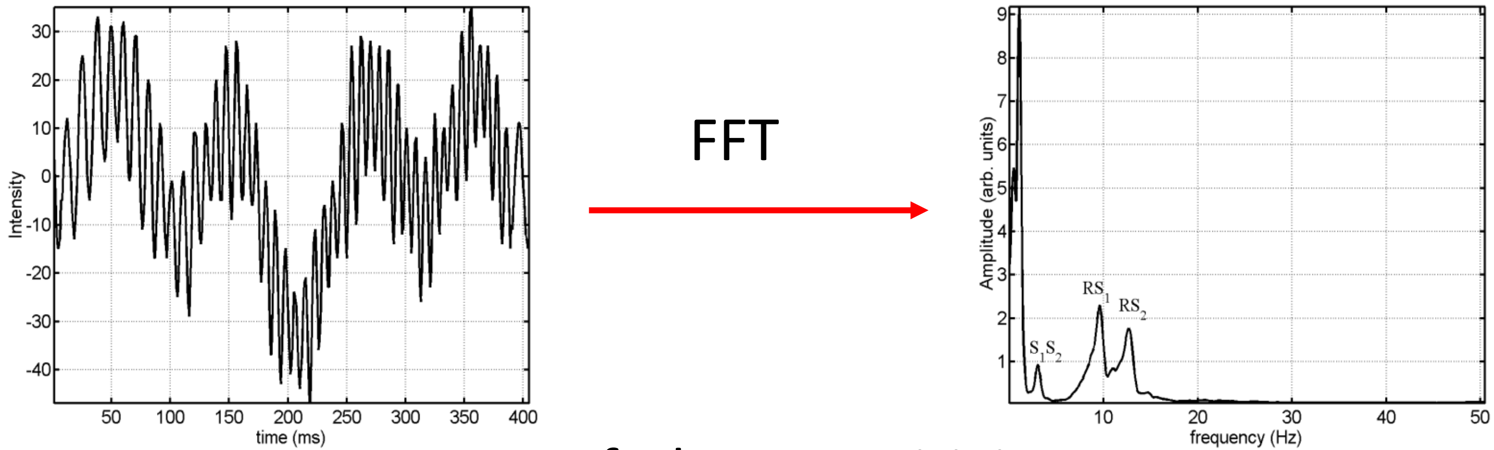

Out-of-plane sensitivity

P. D. Ruiz, J. M. Huntley, and R. D. Wildman, Applied Optics **44**, 3945 (2005)

WSI vs. Speckle Interferometry

WSI

DSPI

Surface S_1

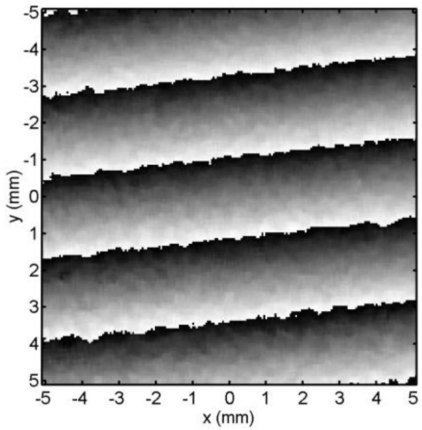

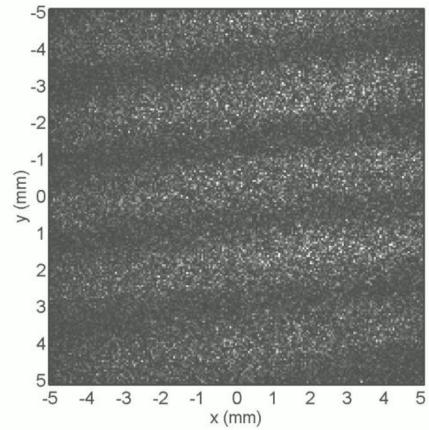

Surface S_1

Surface S_2

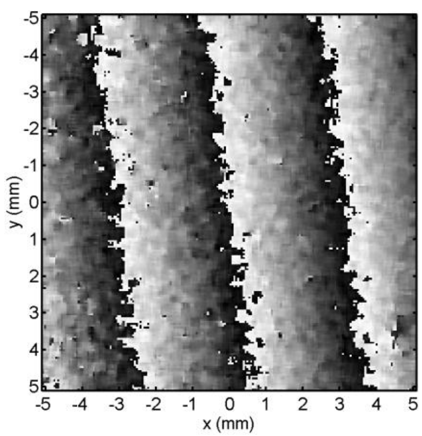

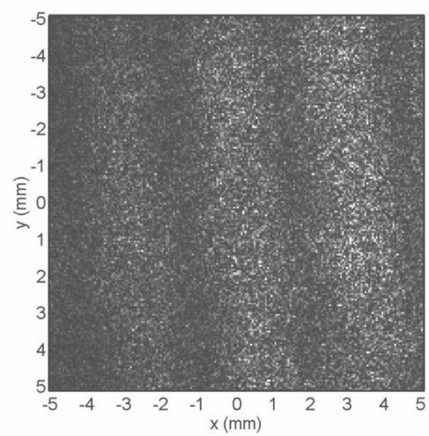

Surface S_2

Depth resolution, range and sensitivity

$$\delta z = \gamma \frac{\lambda_c^2}{\Delta\lambda}$$

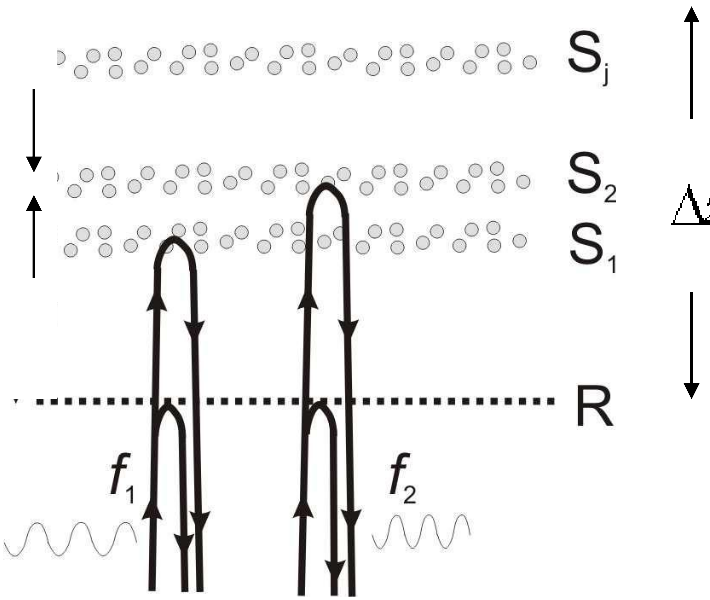

$$\Delta z = \frac{N\lambda_c^2}{4\Delta\lambda}$$

Diode laser
λ_c~635nm
$\Delta\lambda$~0.06nm
N~1000 frames
δz~14mm
Δz~1.7m

P. D. Ruiz et al (2005) *Applied Optics* 44 (19):3945-3953

Current efforts: 1) Multi-axis WSI

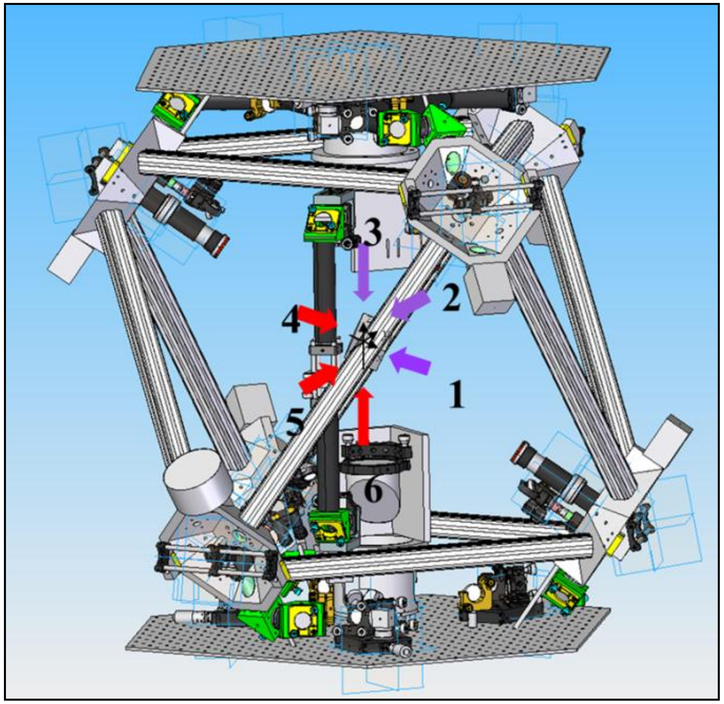

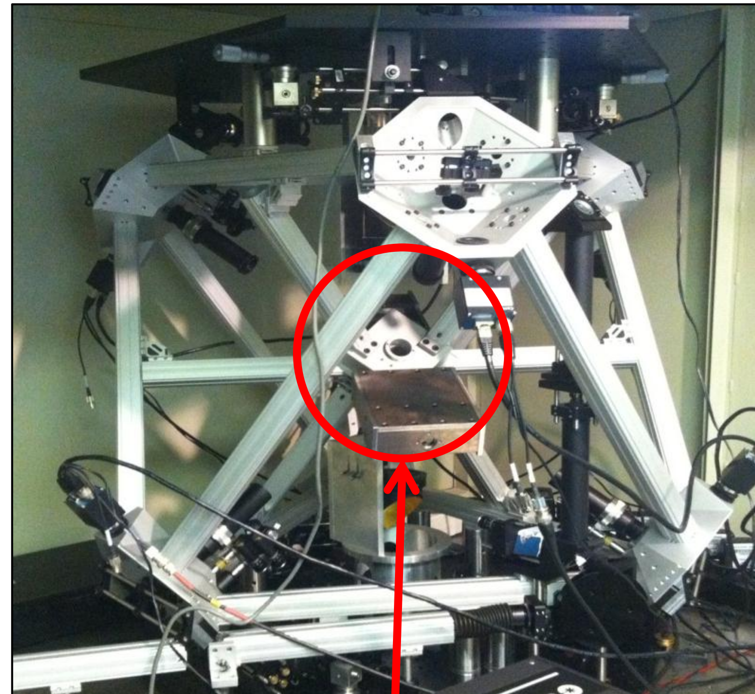

- 6 CCD cameras, >50000 frames each, 30 fps
- Measurement volume: $< 10\times10\times10\ mm^3$
- Ti:Sapphire tunable laser (special specs)
- Depth resolution $\sim10\mu m$
- Displacement sensitivity ~50nm

Loading Rig

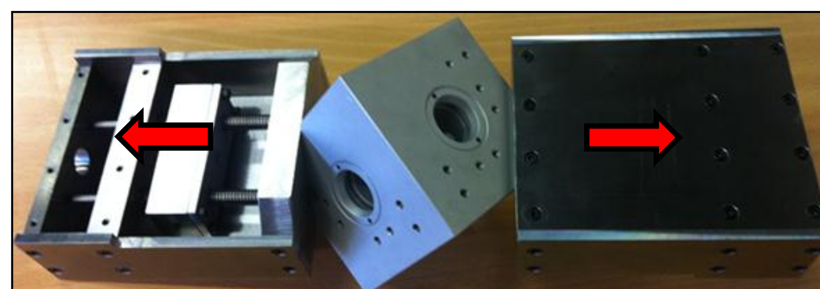

Multi-axis WSI: light source

Example: Coherent MBR Ti:Sa lasers range

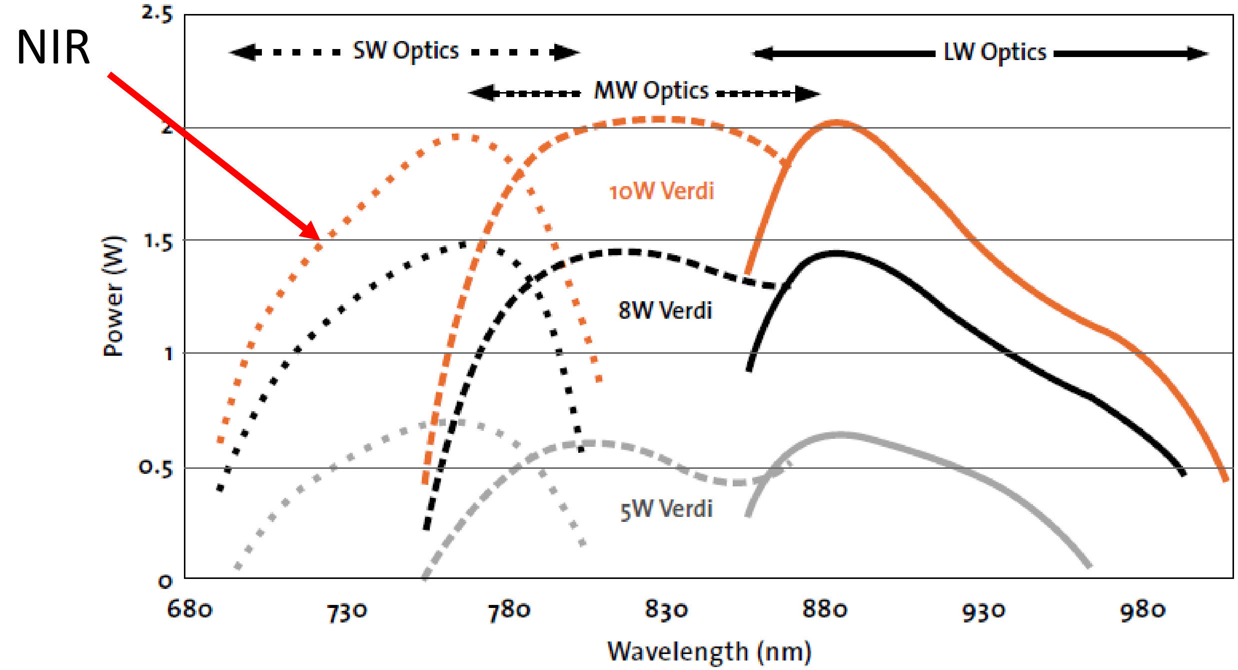

typical NIR , $\Delta\lambda = 150\,nm \;\Rightarrow\; \delta z = 8\mu m$ possible

- No commercially available tuneable light sources with: 1) broad bandwidth, 2) *repeatability* and 3) *stability* (no modes hopes) for direct application to WSI

Multi-axis WSI: light source

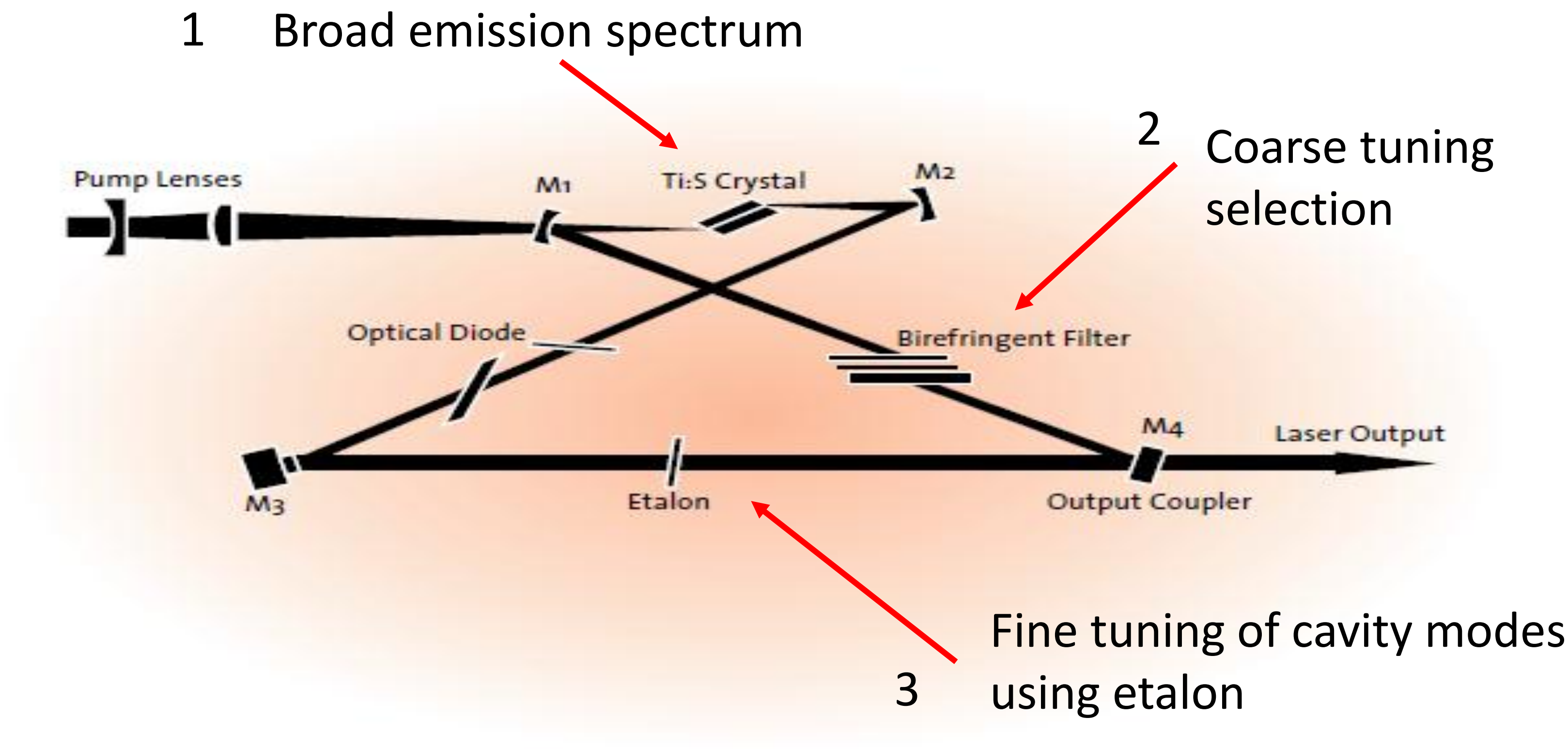

MBR-EL Typical Performance with Verdi Pump Sources

Modes hops and gaps during wavelength scan. Needs substantial post-processing!!

Another approach

- Multiple illumination directions
- One camera

WSI with multiple illumination directions

- **3 illumination directions with offset OPDs**

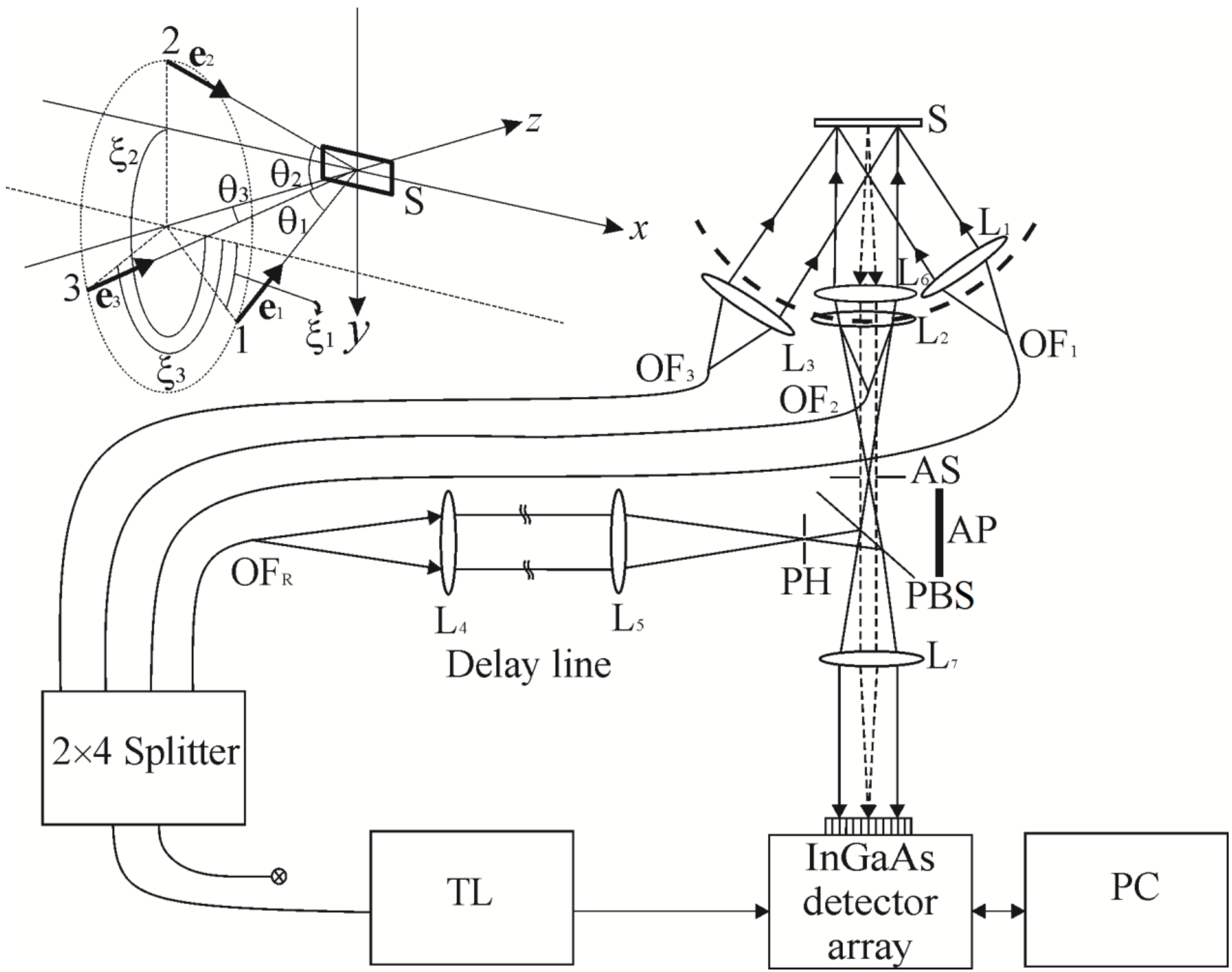

WSI with multiple illumination directions

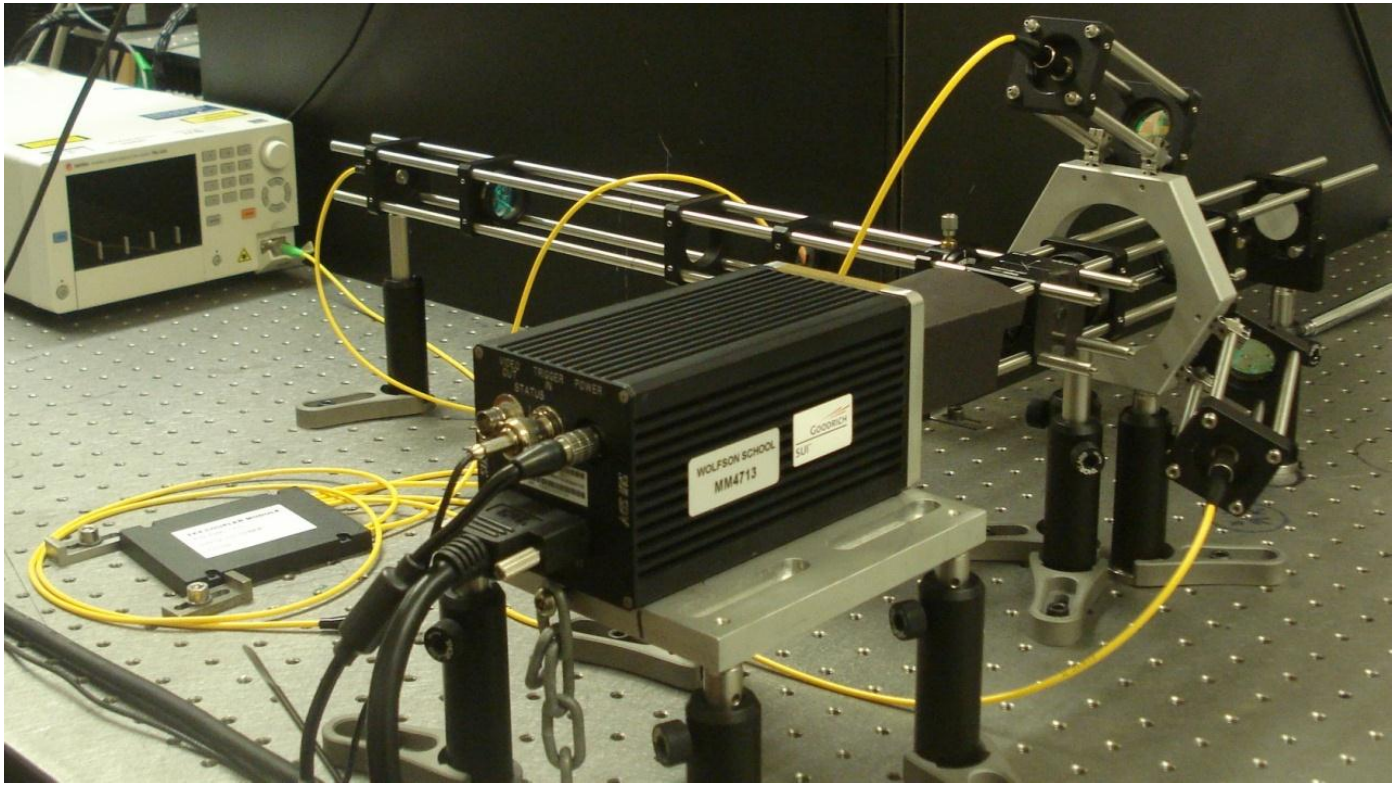

Full paper:

Chakraborty, S. and P.D. Ruiz, J. Opt. Soc. Am. A, 2012. **29**(9): p. 1776-1785.

Opaque surface, one illumination beam

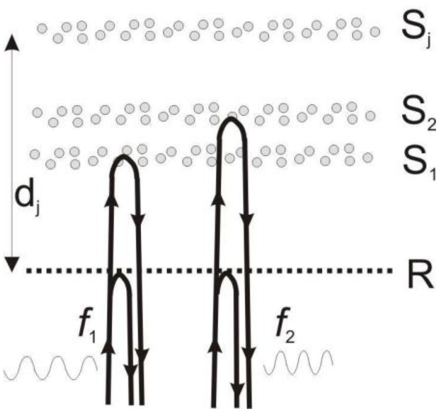

$$I(x,y,k) = I_0(x,y) + I_1(x,y)\cos[\phi(k)]$$

$$k(t) = k_c + \delta k t$$

$$\phi_j(m,n,t) = \phi_{sj}(m,n) + k_c\Lambda_j(m,n) + \delta k \Lambda_j(m,n)t$$

$$f_j(m,n) = \frac{N\delta k}{2\pi}\Lambda_j(m,n)$$

Frequency units in cycles per scan, i.e. FFT index!

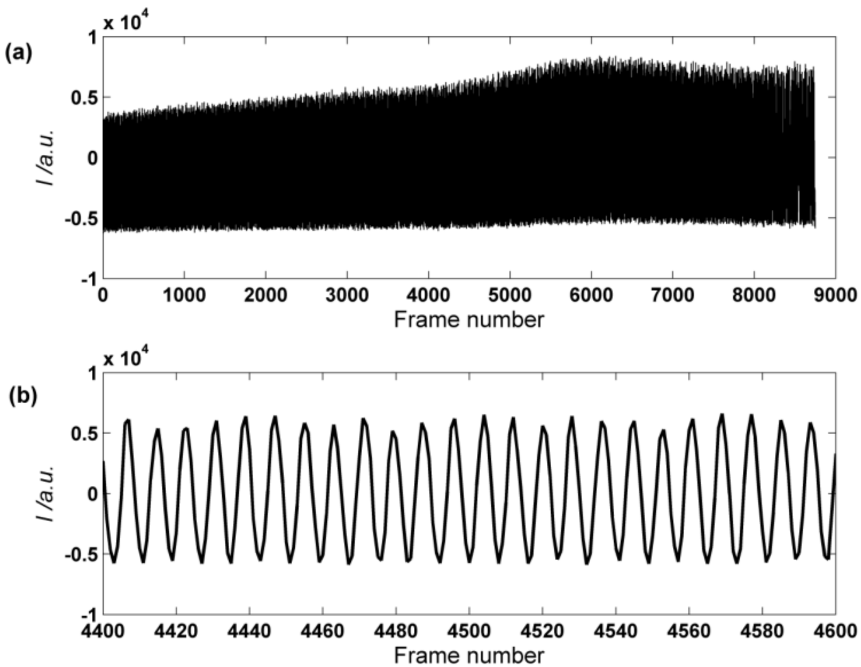

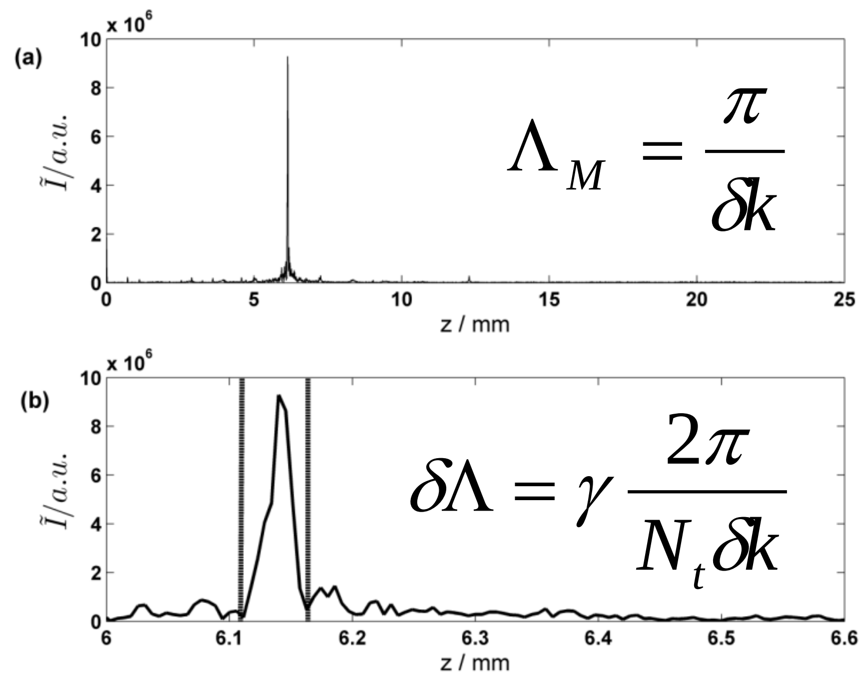

$$\Lambda_M = \frac{\pi}{\delta k}$$

$$\delta\Lambda = \gamma \frac{2\pi}{N_t \delta k}$$

WSI with multiple illumination directions

Signal for the case of an **opaque** surface

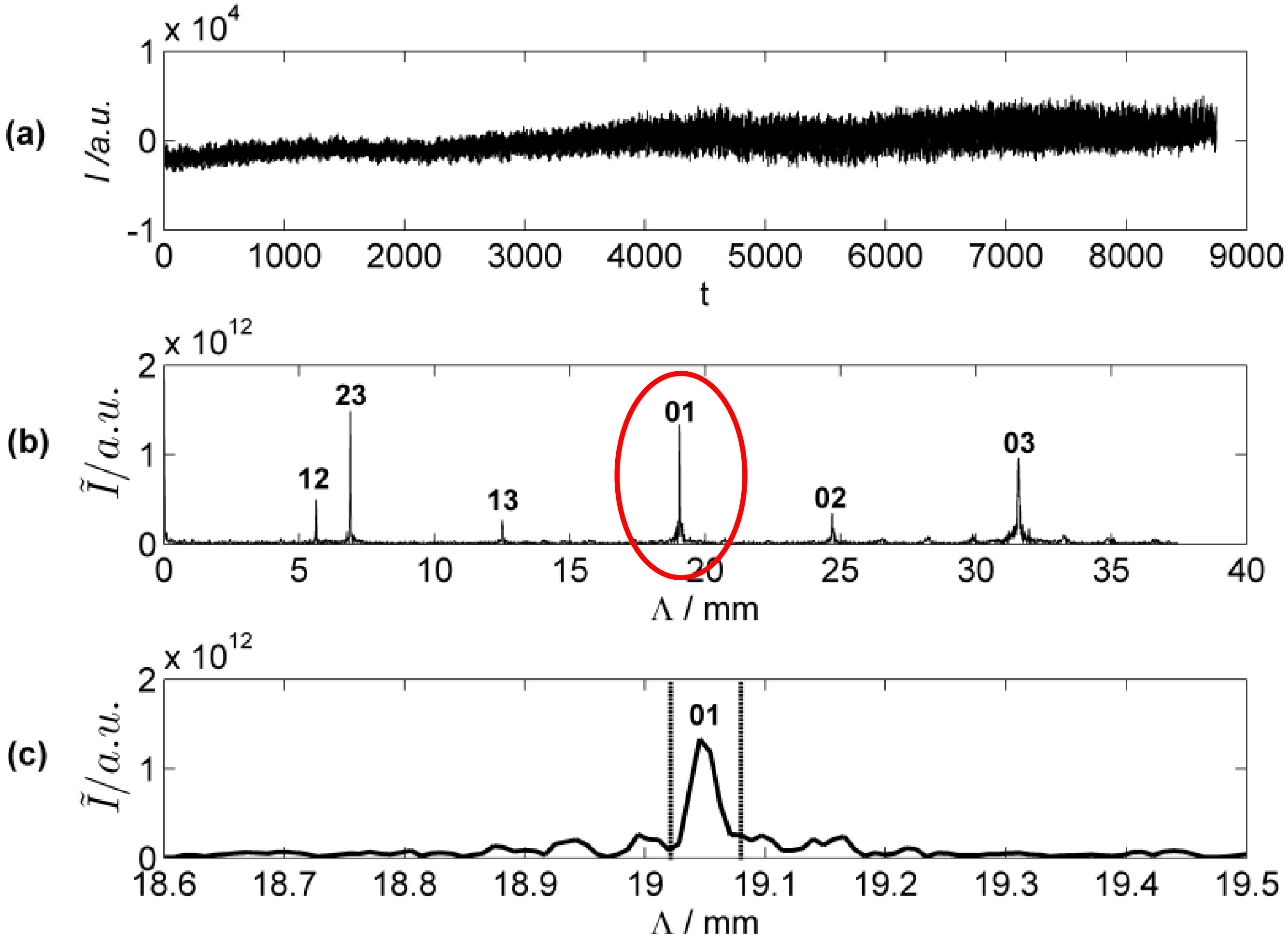

Theoretical $\delta\Lambda$=68 μm; measured $\delta\Lambda$ = 70 μm

Evaluation of the Sensitivity matrix

- Flat opaque scattering surface used as datum
- Record full scan and perform pixel-wise FFT
- Orientation of the reconstructed surfaces for each illumination is used to evaluate illumination and sensitivity vectors

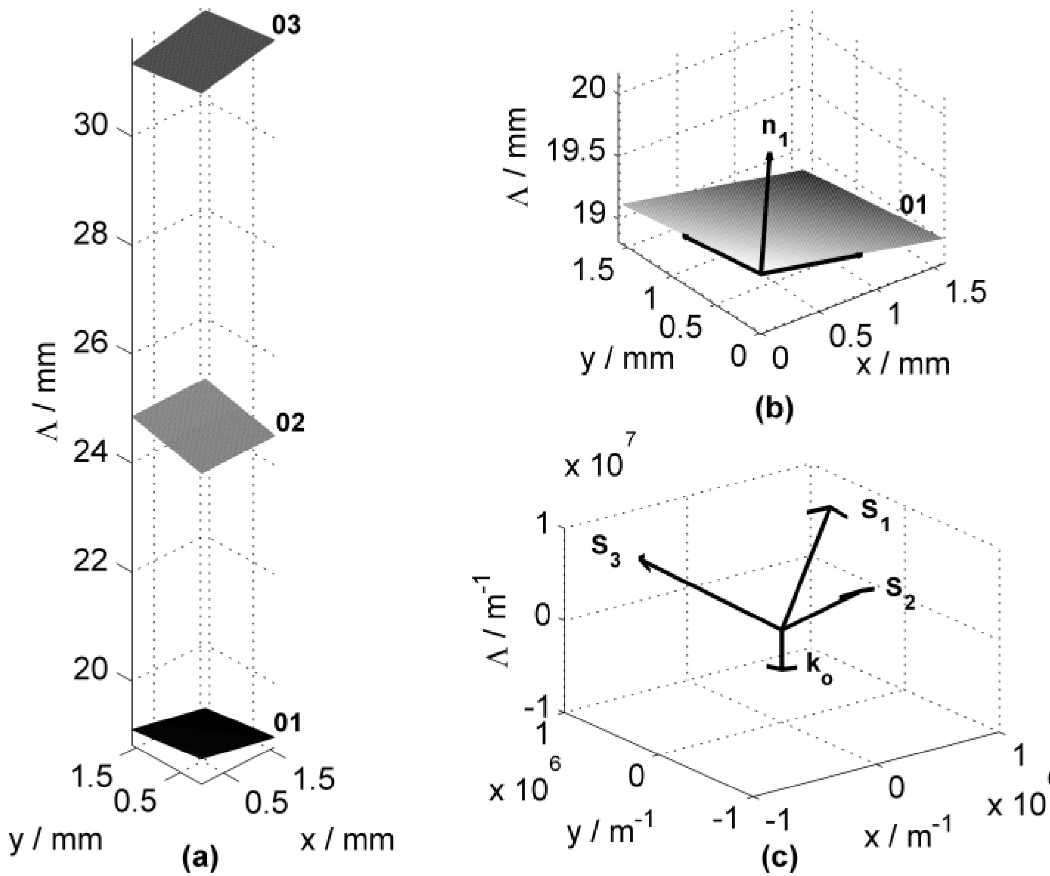

Evaluation of the Sensitivity matrix

Measured from reconstructed flat surface

$$\mathbf{n}_p = \begin{pmatrix} \sin\alpha_p \cos\beta_p \\ \sin\alpha_p \sin\beta_p \\ \cos\alpha_p \end{pmatrix}$$

$$\mathbf{k}_p = \frac{2\pi}{\lambda} \begin{pmatrix} \sin\theta_p \cos\xi_p \\ \sin\theta_p \sin\xi_p \\ \cos\theta_p \end{pmatrix}$$

Sensitivity vectors

$$\mathbf{S}_p = \mathbf{k}_p - \mathbf{k}_o$$

p = 1, 2, 3 (illumination beams)

Volume reconstruction: 1) Re-registration

- The complex volumes associated to all 3 sensitivity vectors are re-registered to a common coordinate system.

S_1 S_2 S_3

Magnitude (microstructure)

Phase (displacements)

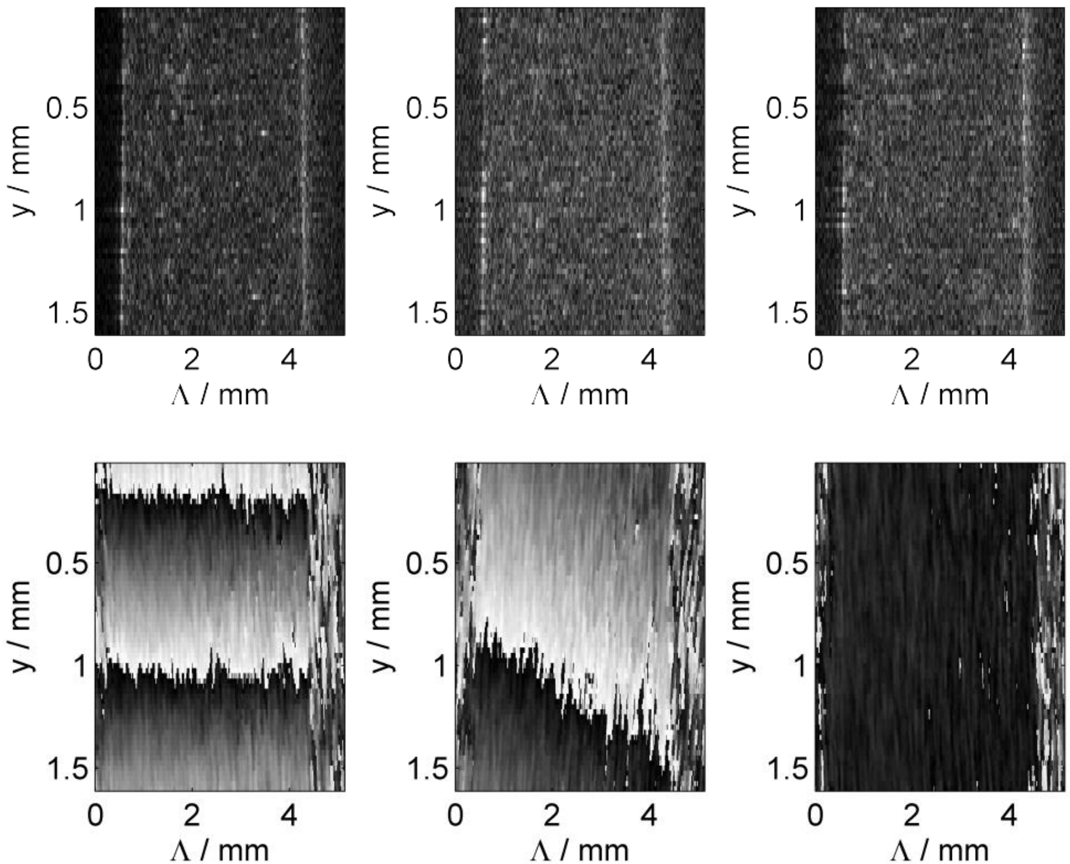

$\phi_1(x, y, \Lambda)$ $\phi_2(x, y, \Lambda)$ $\phi_3(x, y, \Lambda)$

2) phase unwrapping and displacements

$$\begin{pmatrix} \phi_1^U(x,y,\Lambda) \\ \phi_2^U(x,y,\Lambda) \\ \phi_3^U(x,y,\Lambda) \end{pmatrix} = \frac{2\pi}{\lambda_c} \begin{pmatrix} \sin\theta_1 \cos\xi_1 & \sin\theta_1 \sin\xi_1 & 1+\cos\theta_1 \\ \sin\theta_2 \cos\xi_2 & \sin\theta_2 \sin\xi_2 & 1+\cos\theta_2 \\ \sin\theta_3 \cos\xi_3 & \sin\theta_3 \sin\xi_3 & 1+\cos\theta_3 \end{pmatrix} \begin{pmatrix} u(x,y,\Lambda) \\ v(x,y,\Lambda) \\ w(x,y,\Lambda) \end{pmatrix}$$

$$\Phi = \mathrm{S} \cdot \Delta \mathrm{r}$$

u, *v* and *w* are obtained by inverting the sensitivity matrix

Unwrapping algorithm:

Salfity, M.F., et al., Applied Optics, 2006. **45**(12): p. 2711-2722.

Validation of *u*(*x*, *y*, *z*); *v*(*x*, *y*, *z*) and *w*(*x*, *y*, *z*)

Out-of-plane tilt and **In-plane** rotation of object

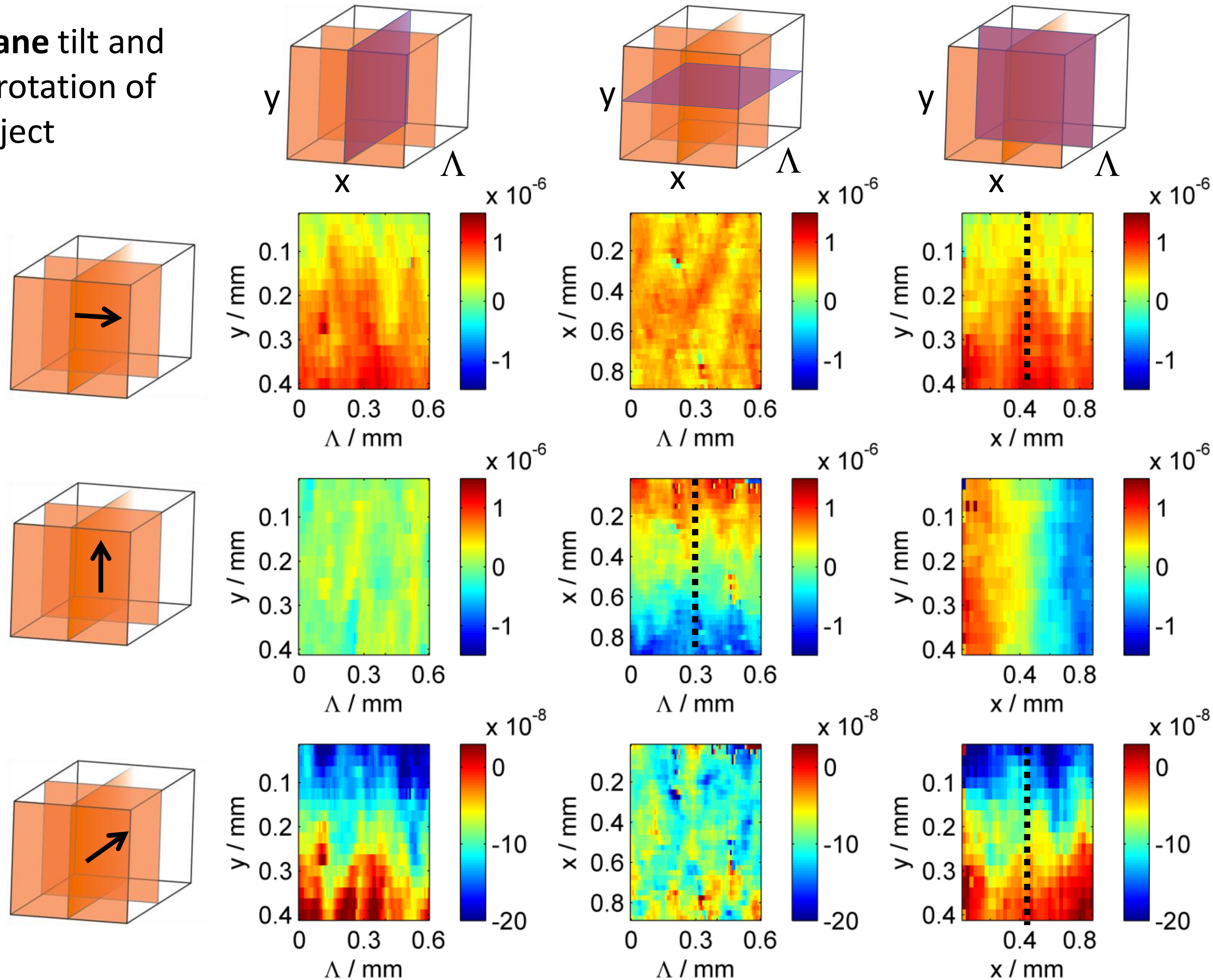

Validation results

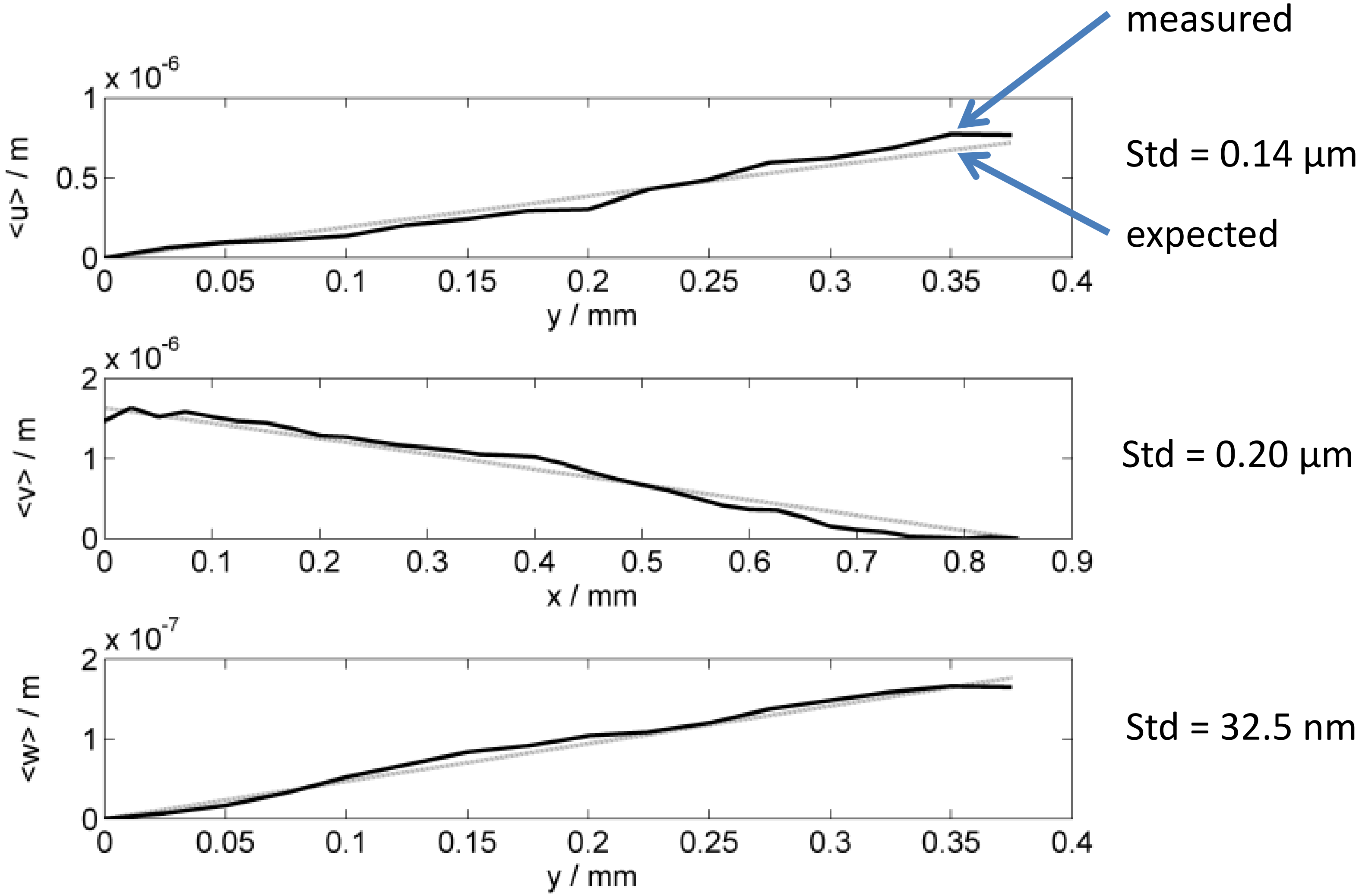

Current challenges

We want the **displacement** of the scattering centres

Surface curvature and geometric distortions

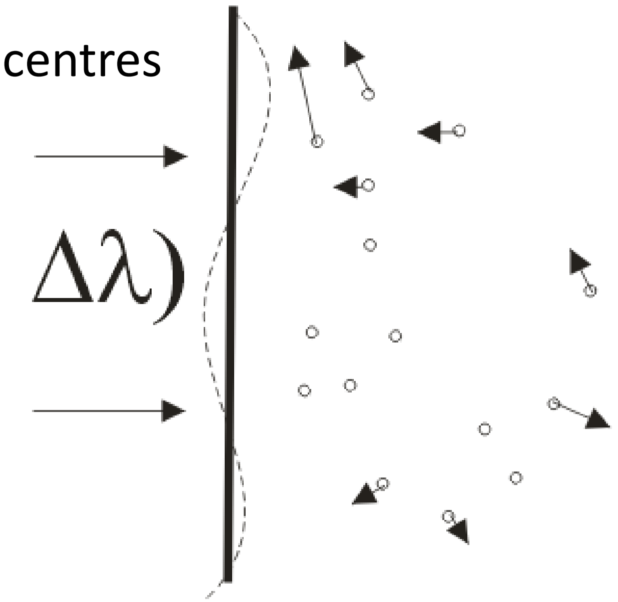

$(\lambda, \Delta\lambda)$

Photoelastic effect $n=f(\varepsilon_1-\varepsilon_2)$

Non-uniform refractive index $n(x, y, z)$

Dispersion $n=f(\lambda)$

Speckle decorrelation and object motion (vibration)

3D phase unwrapping!! Phase sensitive OCT techniques require robust algorithms.

Video [summary]

Acknowledgements

- Prof. Jonathan Huntley
- Dr. Manuel de la Torre-Ibarra
- Dr. Abundio Davila
- Semanti Chakraborty
- Christos Pallikarakis
- Martin Salfity (graphic animation)

Funding

  - EPSRC
  - Wolfson School, LU, (PhD scholarship)

EXTRA SLIDE: phase unwrapping and displacements

- 3D algorithm based on singularity loops and branch surfaces.
- Unwrapping errors limit the size of the measurement volume

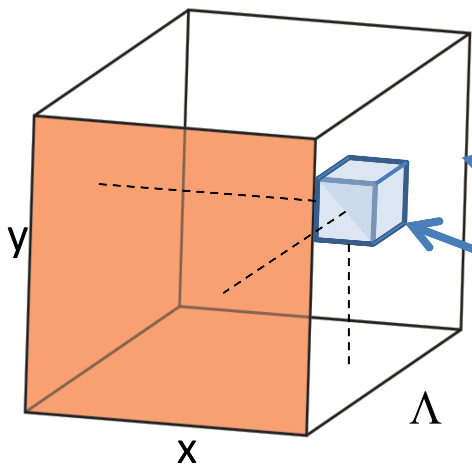

Volume size	Voxels	mm^3
Measured	64 × 64 × 350	~1.6 × 1.8 × 4.5
Unwrapping error free	**16 × 35 × 71**	**~0.4 × 0.9 × 0.9**
Maximum possible	512 × 640 × 3600 **800 times larger!**	~16 × 28 × 62

EXTRA SLIDE: The strain tensor

$$\varepsilon_{ij} = \frac{1}{2}\left(\frac{\partial u_i}{\partial x_j} + \frac{\partial u_j}{\partial x_i}\right)$$

Strain tensor components

$\varepsilon_{11} = \frac{\partial u_1}{\partial x_1}$	$\varepsilon_{12} = \frac{1}{2}\left(\frac{\partial u_1}{\partial x_2} + \frac{\partial u_2}{\partial x_1}\right)$	$\varepsilon_{13} = \frac{1}{2}\left(\frac{\partial u_1}{\partial x_3} + \frac{\partial u_3}{\partial x_1}\right)$
$\varepsilon_{21} = \frac{1}{2}\left(\frac{\partial u_2}{\partial x_1} + \frac{\partial u_1}{\partial x_2}\right)$	$\varepsilon_{22} = \frac{\partial u_2}{\partial x_2}$	$\varepsilon_{23} = \frac{1}{2}\left(\frac{\partial u_2}{\partial x_3} + \frac{\partial u_3}{\partial x_2}\right)$
$\varepsilon_{31} = \frac{1}{2}\left(\frac{\partial u_3}{\partial x_1} + \frac{\partial u_1}{\partial x_3}\right)$	$\varepsilon_{32} = \frac{1}{2}\left(\frac{\partial u_3}{\partial x_2} + \frac{\partial u_2}{\partial x_3}\right)$	$\varepsilon_{33} = \frac{\partial u_3}{\partial x_3}$